

NOTES AND CORRESPONDENCE

Effect of Sea Surface Temperature–Wind Stress Coupling on Baroclinic Instability in the Ocean

MICHAEL A. SPALL

Department of Physical Oceanography, Woods Hole Oceanographic Institution, Woods Hole, Massachusetts

(Manuscript received 8 February 2006, in final form 11 August 2006)

ABSTRACT

The impact of the observed relationship between sea surface temperature and surface wind stress on baroclinic instability in the ocean is explored using linear theory and a nonlinear model. A simple parameterization of the influence of sea surface temperature on wind stress is used to derive a surface boundary condition for the vertical velocity at the base of the oceanic Ekman layer. This boundary condition is applied to the classic linear, quasigeostrophic stability problem for a uniformly sheared flow originally studied by Eady in the 1940s. The results demonstrate that for a wind directed from warm water toward cold water, the coupling acts to enhance the growth rate, and increase the wavelength, of the most unstable wave. Winds in the opposite sense reduce the growth rate and decrease the wavelength of the most unstable wave. For representative coupling strengths, the change in growth rate can be as large as $\pm O(50\%)$. This effect is largest for shallow, strongly stratified, low-latitude flows.

1. Introduction

Recent satellite observations have revealed a clear coupling between the sea surface temperature (SST) and surface wind (Liu et al. 2000; Chelton et al. 2001, 2004; Xie 2004, and the references therein). The sense of this coupling is such that the surface winds are enhanced over regions of warm water and reduced over cold water. This correlation is found over spatial scales of 25–1000 km, at low and midlatitudes, and over time scales ranging from days to long-term means (Chelton et al. 2004; Xie 2004). Proposed mechanisms for this coupling include a downward mixing of momentum from the top of the boundary layer (Sweet et al. 1981; Wallace et al. 1989), secondary circulations driven by cross-front pressure gradients (Lindzen and Nigam 1987; Wai and Stage 1989; Small et al. 2003), and a large-scale adjustment of the pressure gradient in the boundary layer (Samelson et al. 2006).

The basic mechanism by which the atmosphere or

ocean can generate variability through baroclinic conversion of mean potential energy into eddy energy is well described by the seminal work of Eady (1949). Blumsack and Gierasch (1972) extended this flat bottom model to consider the effects of a sloping bottom. They showed that a bottom slope in the opposite direction as the interior sloping isopycnals stabilizes the flow; moderate bottom slopes in the same direction as the isopycnals could enhance the growth rate, but sufficiently strong slopes in this direction would also ultimately stabilize the flow. The wavelength of the most unstable wave is also altered by consideration of bottom topography. The bottom slope affects the characteristics of the unstable waves because the waves have a velocity component across the topography, which forces vertical motion at the lower boundary. This alters the relative vorticity of the flow through conservation of potential vorticity and, as a result, alters the growth characteristics of the waves.

The transport in the oceanic Ekman layer is proportional to the wind stress, and the wind stress curl due to SST gradients can be very large in the vicinity of ocean fronts (Chelton et al. 2004). This implies a relationship between surface temperature and vertical motions at the base of the Ekman layer, and suggests that the

Corresponding author address: Michael A. Spall, Department of Physical Oceanography, Woods Hole Oceanographic Institution, Woods Hole, MA 02543.
E-mail: mspall@whoi.edu

growth of baroclinic waves may be affected by the air–sea coupling, analogous to the effect found for a sloping bottom. The purpose of this note is to explore this coupling in its simplest context, and to identify the relevant parameter that quantifies its influence on the growth of baroclinic waves in the ocean.

2. The Eady model with air–sea coupling

Although the mechanism by which the sea surface temperature alters the surface winds is still a subject of some debate, for the purposes of the present note the details are unimportant and it will be assumed that such a coupling exists. Chelton et al. (2004) and O’Neill et al. (2005) find a nearly linear relationship between the gradient in sea surface temperature and the gradient in surface wind stress in many regions of strong SST gradients. The strength of this coupling is from 1×10^{-2} to $2 \times 10^{-2} \text{ kg m}^{-1} \text{ s}^{-2} \text{ }^\circ\text{C}^{-1}$ and has been found to be similar across a wide range of ocean currents.

This relationship may be used to represent the SST/wind stress coupling in the Eady model of baroclinic instability through the surface boundary condition. Consider a quasigeostrophic (QG) ocean with uniform vertical shear in zonal velocity and uniform stratification. The initial SST gradient is then uniform in the meridional direction and zero in the zonal direction. Although the present analysis is on an f plane, and hence does not depend on the orientation of the flow, for convenience it will be assumed that the mean flow is zonal. It is assumed that there is a background meridional wind stress with zero curl directed along the SST gradient (across the mean ocean flow). Growing perturbations that have a wavelike structure in the zonal direction will displace the SST contours in the meridional direction such that zonal gradients in sea surface temperature will develop. The air–sea coupling will result in regions of enhanced wind stress over warm water and reduced wind stress over cold water. A schematic of such a flow situation is shown in Fig. 1 for a background wind from warm water toward cold water. The Ekman transport associated with these perturbations to the wind is zonal, and will drive regions of upwelling and downwelling, w_E , that are directly related to the zonal gradients in SST as

$$w_E = \frac{\gamma T_x}{\rho_0 f}, \tag{1}$$

where T_x is the zonal SST gradient, ρ_0 is a representative ocean density, f is the Coriolis parameter, and $\gamma = \partial\tau/\partial T$, where $\tau > 0$ for background wind from warm to cold SST. If the background wind is from warm water

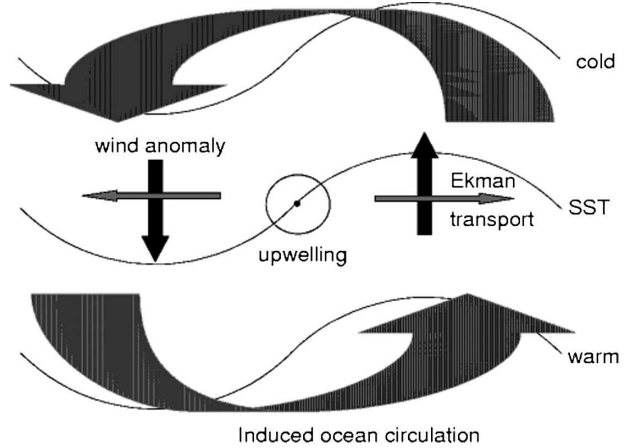


FIG. 1. Schematic of a growing wave with background winds from warm to cold SST. Small perturbations in SST result in wind anomalies that drive divergent Ekman transport, upwelling, and a cyclonic ocean circulation anomaly. This circulation advects warm water northward and cold water southward, which in turn leads to larger SST anomalies and enhances the growth rate of the wave.

toward cold water $\gamma > 0$, and if the wind is in the opposite direction, $\gamma < 0$.

The starting point is the quasigeostrophic potential vorticity equation, with the variables nondimensionalized using $(x', y') = L(x, y)$, $z' = Hz$, $\mathbf{v}' = U\mathbf{v}$, and $t' = (L/U)t$, where primes denote dimensional variables. A streamfunction is introduced such that the geostrophic velocity $\mathbf{v} = \mathbf{k} \times \nabla\psi$, and $\psi' = \rho_0 U f L \psi$. The temperature consists of a uniform background stratification and a perturbation due to the motion, $T = T_0[z + (\epsilon/B)\tilde{T}(x, y, z, t)]$, where $\epsilon = U/(fL)$ is the Rossby number and $B = [NH/(fL)]^2$ is the Burger number. The density is linearly related to temperature as $\rho = \rho_0 - \alpha T$, and the streamfunction is related to density through the hydrostatic relation.

The derivation of the nondimensional quasigeostrophic equations follows the standard approach as found, for example, in Blumsack and Gierasch (1972), with the vertical velocity at the surface given by (1). Conservation of potential vorticity in the interior of the fluid is expressed as

$$\left(\frac{\partial}{\partial t} + \mathbf{v} \cdot \nabla\right) \left(\nabla^2 + \frac{1}{B} \frac{\partial^2}{\partial z^2}\right) \psi = 0. \tag{2}$$

Surface and bottom boundary conditions are

$$\left(\frac{\partial}{\partial t} + \mathbf{v} \cdot \nabla\right) \psi_z + \delta\psi_{xz} = 0 \quad \text{at } z = 1 \quad \text{and} \tag{3}$$

$$\left(\frac{\partial}{\partial t} + \mathbf{v} \cdot \nabla\right) \psi_z = 0 \quad \text{at } z = 0. \tag{4}$$

The boundary conditions arise from the conservation of density at the boundary. The second term in (3) expresses the change in density due to the vertical advection of the mean stratification by the Ekman pumping velocity. This term is similar to that resulting from a sloping bottom but is proportional to ψ_{xz} instead of ψ_x , or temperature gradient instead of meridional velocity, because the Ekman pumping velocity is driven by the zonal temperature gradient. The strength of the SST–wind stress coupling is given by $\delta = \gamma N^2 / \alpha g f U$, where N^2 is the Brunt–Väisälä frequency and g is the gravitational acceleration. The coupling parameter may also be written as $\delta = \gamma N^2 / \alpha g H S^2$, where $S^2 = U f l H$ is a measure of the horizontal stratification.

The influence of the coupling, represented by δ , depends on two things: the SST anomaly and the atmospheric response to that anomaly. The atmospheric response is measured by γ , taken from the satellite observations of Chelton et al. (2004) and O’Neill et al. (2005). The change in SST due to coupling depends on the vertical velocity and the stratification. Increasing N^2 increases the coupling because it results in a larger change in SST for a given vertical velocity. The coupling depends inversely on f because the vertical Ekman pumping velocity, for a given wind stress, depends inversely on f . The coupling decreases with increasing horizontal velocity scale U because this term is scaled relative to the lateral advection term.

The streamfunction for a uniformly sheared zonal mean flow with a small perturbation $\phi \ll 1$ may be written as $\psi = -yz + \phi$. The linearized potential vorticity equation for the perturbation is

$$\left(\frac{\partial}{\partial t} + z \frac{\partial}{\partial x} \right) \left(\nabla^2 \phi + \frac{1}{B} \frac{\partial^2 \phi}{\partial z^2} \right) = 0 \quad (5)$$

with surface and bottom boundary conditions

$$\left[\frac{\partial}{\partial t} + (1 + \delta) \frac{\partial}{\partial x} \right] \phi_z - \phi_x = 0 \quad \text{at } z = 1 \quad \text{and} \quad (6)$$

$$\frac{\partial \phi_z}{\partial t} - \phi_x = 0 \quad \text{at } z = 0. \quad (7)$$

It is assumed that the perturbation is wavelike in x and is an as yet undetermined function of z :

$$\phi = F(z) e^{i(kx - \sigma t)}. \quad (8)$$

This gives rise to an eigenvalue problem for the wavenumber, frequency, and vertical structure of the waves. The equation to be solved is

$$(-\sigma + zk)(-k^2 F + B^{-1} F_{zz}) = 0 \quad (9)$$

with boundary conditions

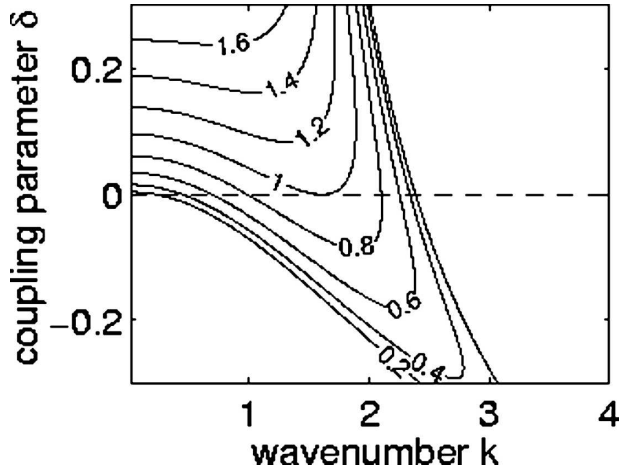


FIG. 2. Theoretical growth rate from (13), normalized by the maximum growth rate for the uncoupled Eady problem, as a function of wavenumber k and coupling parameter δ .

$$-\sigma F_z - kF = 0 \quad \text{at } z = 0 \quad \text{and} \quad (10)$$

$$[-\sigma + (1 + \delta)k]F_z - kF = 0 \quad \text{at } z = 1. \quad (11)$$

The solution to the above set of equations is

$$\phi = A e^{i(kx - \sigma t)} [\sinh(\mu z) - \eta \cosh(\mu z)], \quad (12)$$

where $\mu = kB^{1/2}$, $\eta = \sigma B^{1/2}$, and A is an arbitrary amplitude. The eigenvalue η is given by

$$\eta = \frac{\mu}{2} (1 + \delta) \pm \left[\frac{\mu^2}{4} (1 + \delta)^2 - \frac{\mu(1 + \delta) - \tanh(\mu)}{\tanh(\mu)} \right]^{1/2}. \quad (13)$$

If the second term in (13) is imaginary, the flow will support exponentially growing waves. The growth rate of the most unstable wave, normalized by the maximum growth rate for the uncoupled Eady problem, is shown in Fig. 2 as a function of the coupling parameter δ and the wavenumber k . The standard Eady problem is recovered for $\delta = 0$. Winds directed from warm water toward cold water ($\delta > 0$) enhance the growth rate for long waves, while winds from cold to warm decrease the growth rate of the long waves. The opposite trend is found for very short waves, where they can be destabilized by winds blowing from cold to warm water. The wavenumber of the most unstable wave decreases for $\delta > 0$ and increases for $\delta < 0$. The coupling most strongly affects the longest waves, where the growth rate increases as $\delta^{1/2}$. For weak coupling, the growth rate of the most unstable wave increases approximately linearly with δ as

$$\eta_i \approx \eta_0 + 0.5 \eta_0^{-1/2} \left[\frac{\mu_0}{\tanh(\mu_0)} - 0.5 \mu_0^2 \right] \delta, \quad (14)$$

where η_0 and μ_0 are the values for the most unstable wave with $\delta = 0$. For waves near the deformation radius, $\eta_i/\eta_0 \approx 1 + 2.35\delta$. The growth rate varies by approximately 50% relative to the uncoupled case for $\delta = \pm 0.2$.

The mechanism responsible for the coupling influence on the growth of the waves is fairly straightforward. Consider a wind blowing toward the north over an eastward mean flow ($\delta > 0$), as depicted in Fig. 1. The coupling (1) will force upwelling between a wave trough to the west and crest to the east, which will then enhance the cyclonic vorticity in order to conserve potential vorticity. The sense of this circulation is to further push the crest of the wave poleward and the trough of the wave equatorward. This has a positive feedback by increasing the SST anomaly and thus enhances the growth rate of the wave. The opposite situation results if the winds are from the cold water toward the warm water. This drives downwelling in regions of positive zonal SST gradient and anticyclonic vorticity, tending to reduce the SST anomaly. The wind component along the direction of the mean ocean flow does not alter the growth rate of the waves because the phase relationship between the Ekman pumping and the growing waves does not lead to positive feedback. The full situation is more complicated than this, involving wave propagation and advection of SST by the mean and perturbation flows, but this simple framework serves to illustrate the basic process.

The first term in (13) represents the real part of the frequency and relates to the phase speed of the wave. The coupling increases the phase speed for $\delta > 0$ and decreases the phase speed for $\delta < 0$. The mechanism behind this influence is clear from the schematic in Fig. 1. The dimensional phase speed of the uncoupled wave is $U/2$ and directed toward the east. For $\delta > 0$, the cooling of SST due to Ekman suction leads the trough of the wave by one-quarter wavelength. This is in phase with the tendency due to lateral advection by the mean flow, and effectively increases the propagation of the temperature signal. For $\delta < 0$, the Ekman pumping warms the surface and acts opposite to the tendency due to lateral advection by the mean flow, decreasing the phase speed of the wave.

3. Nonlinear model calculations

The Regional Oceanic Modeling System (ROMS) primitive equation numerical model (Shchepetkin and McWilliams 2005) has been run to compare with this linear theory. The model is configured in a periodic channel of length and width 1000 km with horizontal grid spacing of 5 km. The depth of the channel is 500 m,

and the model uses 25 uniformly spaced levels in the vertical direction. The Coriolis parameter $f = 10^{-4} \text{ s}^{-1}$. The model incorporates lateral viscosity and diffusivity with coefficients $20 \text{ m}^2 \text{ s}^{-1}$ and a vertical viscosity and diffusivity of $10^{-5} \text{ m}^2 \text{ s}^{-1}$. The internal deformation radius is 25 km, which, with the above depth and Coriolis parameter, gives $N^2 = 2.5 \times 10^{-5} \text{ s}^{-2}$.

The model is forced at the surface with a meridional wind stress that is proportional to the temperature anomaly as

$$\tau(x, y, t) = \gamma[T(x, y, t) - \bar{T}(y)], \quad (15)$$

where $\bar{T}(y)$ is the initial meridional sea surface temperature profile. This approach neglects the background meridional wind stress that has zero curl. Calculations that include this background wind field give similar results; however, in these cases, the growth of the waves is influenced by the interaction of the mean wind with the channel walls. Since the interest here is the influence of the SST–wind coupling on instability of open-ocean currents, and the focus is on the initial growth rates, this background wind field has been removed. Its neglect may become important for very-large-amplitude temperature anomalies, because (15) assumes that there is always sufficient momentum available in the lower atmosphere to alter the surface winds. A similar linear parameterization of the influence of SST anomalies on wind stress was used in the modeling study of tropical instability waves by Pezzi et al. (2004). They found that the coupling between SST and wind stress reduces the instability of the waves, in qualitative agreement with the influence predicted here.

The horizontal stratification S^2 (or zonal mean velocity) and the strength of the air–sea coupling γ are prescribed by the Rossby number $\epsilon = U/(fL)$ and the coupling coefficient S . In each case reported here, $\epsilon = 0.02$ and the Burger number $B = 1$. The coupling coefficient δ has been varied between ± 0.2 , which, for the above parameters, corresponds to a range for the dimensional coupling coefficient of $\pm 1.6 \times 10^{-2} \text{ kg m}^{-1} \text{ s}^{-2} \text{ }^\circ\text{C}^{-1}$, similar to that inferred from satellite data (Chelton et al. 2004; O’Neill et al. 2005). Note that, for a given dimensional coupling strength, the nondimensional δ increases with increasing vertical stratification, decreasing horizontal stratification, and decreasing depth (or equivalently decreasing U and f). Thus the coupling mechanism affects the growth rate of the waves most strongly for shallow, strongly stratified, weak, low-latitude flows.

The numerical model was initialized with uniform vertical and horizontal stratification and a geostrophically balanced, baroclinic zonal flow and small, random

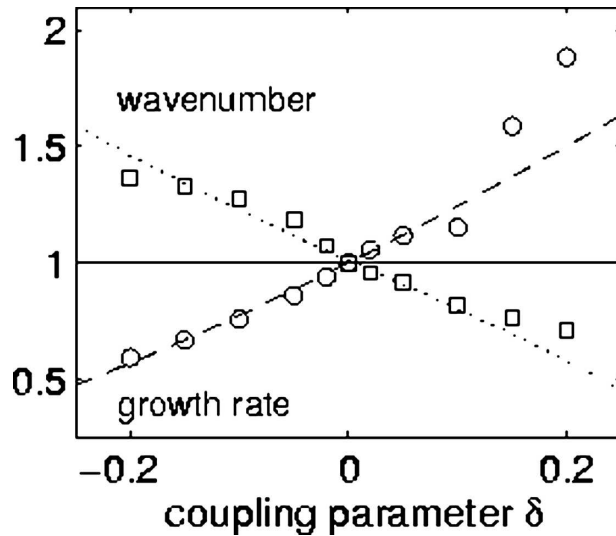


FIG. 3. Growth rate (circles) and wavenumber (squares) of growing wave from the numerical model as a function of the coupling parameter δ . Predictions from the linear theory are given by the dashed and dotted lines. All quantities are normalized by their value for the uncoupled Eady problem.

perturbations in the density field. The growth rate of the perturbations was diagnosed before the waves grew to large amplitude (root-mean-square temperature perturbation less than 0.1°C). In each case, a clear period of exponential growth was identified. The model growth rate is compared with that predicted by (13) in Fig. 3, once again normalized by the growth rate for the $\delta = 0$ case. The model compares reasonably well to the theory, especially for δ small and less than zero. The growth rate in the nonlinear model exceeds that predicted by the theory for $\delta \geq 0.15$.

The wavelength k_0 of the most unstable wave has also been diagnosed from the model runs based on the spectral distribution of temperature variance as

$$k_0 = \frac{\int_0^{k_m} \hat{T} k \, dk}{\int_0^{k_m} \hat{T} \, dk}, \quad (16)$$

where \hat{T} is the spectral density of the temperature variance in the zonal direction at the midlatitude of the basin and $k_m = 100$ is the maximum wavenumber represented in the model. The most unstable wavelength is $O(100 \text{ km})$ for these calculations. The model reproduces the dependence of the wavenumber on the coupling parameter δ (Fig. 3). Wind from warm to cold water, $\delta > 0$, favors longer waves, whereas wind from cold to warm water favors shorter waves.

4. Conclusions

The observed relationship between sea surface temperature and surface wind stress suggests a coupled interaction that might alter the growth rate of baroclinically unstable waves in the ocean. A simple parameterization of that coupling is developed in which the Ekman pumping rate at the ocean surface is related to the lateral gradient of sea surface temperature. This surface boundary condition has been applied to the classic stability problem of Eady (1949) to explore the influence of air–sea coupling on the growth of baroclinic waves. It is shown that winds blowing from warm water toward cold water enhance the growth rate and wavelength of the most unstable wave. Winds blowing from cold water toward warm water have the opposite effect. This mechanism is active for winds with a component in the direction of the sea surface temperature gradient, and is most influential for shallow, strongly stratified flows at low latitudes.

The main intent of this note is to illustrate the basic mechanism of interaction and to quantify the strength of the coupling through the nondimensional parameter δ . There are many situations in which these effects may be important. Air–sea coupling has been observed in the vicinity of tropical instability waves in the eastern Pacific Ocean (Wallace et al. 1989; Liu et al. 2000; Chelton et al. 2001), where the winds have a strong meridional component that, based on the present analysis, will tend to stabilize baroclinic waves. This is qualitatively consistent with the modeling results of Pezzi et al. (2004). Cold outbreaks over the Gulf Stream in winter may also have a stabilizing influence. Cross-frontal winds are also likely to arise in near coastal regions where winds blow off of land over the ocean. Even in situations for which the large-scale winds are generally along the direction of an ocean front, such as the Antarctic Circumpolar Current, the lower Ekman layer in the atmosphere will drive a wind component from the warm side to the cold side of the front, tending to enhance wave growth.

The magnitude of the nondimensional parameter $\delta = \gamma N^2 / (g\alpha f U)$ can be estimated for several of these flow regions. Taking $\gamma = \pm 2 \times 10^{-2} \text{ kg m}^{-1} \text{ s}^{-2} \text{ }^\circ\text{C}^{-1}$ (O'Neill et al. 2005), $\alpha = 2 \times 10^{-1} \text{ kg m}^{-3} \text{ }^\circ\text{C}^{-1}$, and $g = 10 \text{ m s}^{-2}$ as constant, the only parameters that need to be defined are N^2 , f , and U . For the Gulf Stream region, the stratification near the surface is $N^2 = 10^{-4} \text{ s}^{-2}$, $f = 10^{-4} \text{ s}^{-1}$, and $U = 1 \text{ m s}^{-1}$, giving $\delta = 0.01$. The shelfbreak front along the U.S. East Coast has $U = 0.2 \text{ m s}^{-1}$, $f = 10^{-4} \text{ s}^{-1}$, and $N^2 = 10^{-4} \text{ s}^{-2}$ in winter and $N^2 = 4 \times 10^{-4} \text{ s}^{-2}$ in summer (Linder and Gawarkiewicz 1998), giving $\delta = 0.07$ in winter and $\delta = 0.27$ in

summer. The tropical instability waves in the equatorial Pacific have $N^2 = 10^{-4} \text{ s}^{-2}$, $f = 4 \times 10^{-6} \text{ s}^{-1}$, and $U = 0.5 \text{ m s}^{-1}$, giving $\delta = 0.5$. Based on this scaling, the proposed coupling mechanism will be only marginally important for midlatitude separated western boundary currents such as the Gulf Stream or Kuroshio, mainly because their horizontal advection speeds are very large. It is more likely to be important for weaker, shallow midlatitude currents such as shelfbreak jets. It is also may become important for the zonal flows found near the equator, where tropical instability waves are present, keeping in mind that QG theory and the Ekman layer balance become questionable at very low latitudes.

Acknowledgments. This work was supported by the Office of Naval Research Grant N00014-05-1-0300. Comments and suggestions from Roger Samelson, Dudley Chelton, and two anonymous reviewers are gratefully acknowledged.

REFERENCES

- Blumsack, S. L., and P. J. Gierasch, 1972: Mars: The effects of topography on baroclinic instability. *J. Atmos. Sci.*, **29**, 1081–1089.
- Chelton, D. B., and Coauthors, 2001: Observations of coupling between surface wind stress and sea surface temperature in the eastern tropical Pacific. *J. Climate*, **14**, 1479–1498.
- , M. G. Schlax, M. H. Freilich, and R. F. Milliff, 2004: Satellite measurements reveal persistent small-scale features in ocean winds. *Science*, **303**, 978–983.
- Eady, E. T., 1949: Long waves and cyclone waves. *Tellus*, **1**, 33–52.
- Linder, C. A., and G. Gawarkiewicz, 1998: A climatology of the shelfbreak front in the Middle Atlantic Bight. *J. Geophys. Res.*, **103**, 18 405–18 424.
- Lindzen, R. S., and S. Nigam, 1987: On the role of sea surface temperature gradients in forcing low-level winds and convergence in the Tropics. *J. Atmos. Sci.*, **44**, 2418–2436.
- Liu, W. T., X. Xie, P. S. Polito, S.-P. Xie, and H. Hashizume, 2000: Atmospheric manifestation of tropical instability wave observed by QuikSCAT and Tropical Rain Measuring Mission. *Geophys. Res. Lett.*, **27**, 2545–2548.
- O'Neill, L. W., D. B. Chelton, S. K. Esbensen, and F. J. Wentz, 2005: High-resolution satellite measurements of the atmospheric boundary layer response to SST variations along the Agulhas return current. *J. Climate*, **18**, 2706–2723.
- Pezzi, L. P., J. Vialard, K. J. Richards, C. Menkes, and D. Anderson, 2004: Influence of ocean–atmosphere coupling on the properties of tropical instability waves. *Geophys. Res. Lett.*, **31**, L16306, doi:10.1029/2004GL019995.
- Samelson, R. M., E. D. Skillingstad, D. B. Chelton, S. K. Esbensen, L. W. O'Neill, and N. Thum, 2006: On the coupling of wind stress and sea surface temperature. *J. Climate*, **19**, 1557–1566.
- Shchepetkin, A. F., and J. C. McWilliams, 2005: The Regional Oceanic Modeling System (ROMS): A split-explicit, free-surface, topography-following coordinate ocean model. *Ocean Modell.*, **9**, 347–404.
- Small, R. J., S.-P. Xie, and Y. Wang, 2003: Numerical simulation of atmospheric response to Pacific tropical instability waves. *J. Climate*, **16**, 3723–3741.
- Sweet, W., R. Fett, J. Kerling, and P. La Violette, 1981: Air-sea interaction effects in the lower troposphere across the north wall of the Gulf Stream. *Mon. Wea. Rev.*, **109**, 1042–1052.
- Wai, M., and S. Stage, 1989: Dynamical analyses of marine atmospheric boundary layer structure near the Gulf Stream oceanic front. *Quart. J. Roy. Meteor. Soc.*, **115**, 29–44.
- Wallace, J. M., T. P. Mitchell, and C. Deser, 1989: The influence of sea-surface temperature on surface wind in the eastern equatorial Pacific: Seasonal and interannual variability. *J. Climate*, **2**, 1492–1499.
- Xie, S.-P., 2004: Satellite observations of cool ocean–atmosphere interaction. *Bull. Amer. Meteor. Soc.*, **85**, 195–208.